

See discussions, stats, and author profiles for this publication at: <https://www.researchgate.net/publication/324507267>

Comparison of excess heat evolution from zirconia-supported Pd-Ni nanocomposite samples with different Pd/Ni ratio under exposure to hydrogen isotope gases

Preprint · April 2018

CITATIONS

0

READS

208

17 authors, including:



Akira Kitamura
Kobe University

89 PUBLICATIONS 283 CITATIONS

SEE PROFILE



Akito Takahashi
Technova Inc

280 PUBLICATIONS 1,248 CITATIONS

SEE PROFILE



Koh Takahashi
Technova Inc

28 PUBLICATIONS 363 CITATIONS

SEE PROFILE



Yasuhiro Iwamura
Tohoku University

39 PUBLICATIONS 269 CITATIONS

SEE PROFILE

Some of the authors of this publication are also working on these related projects:



Nuclear Data and Neutronics for DT Fusion Reactors [View project](#)



Toyota R&D Laboratories Inc. [View project](#)

Comparison of excess heat evolution from zirconia-supported Pd-Ni nanocomposite samples with different Pd/Ni ratio under exposure to hydrogen isotope gases

Akira Kitamura^{1,5}, Akito Takahashi¹, Koh Takahashi¹, Reiko Seto¹, Takeshi Hatano¹,
Yasuhiro Iwamura², Takehiko Itoh², Jirohta Kasagi²,
Masanori Nakamura³, Masanobu Uchimura³, Hidekazu Takahashi³, Shunsuke Sumitomo³,
Tatsumi Hioki⁴, Tomoyoshi Motohiro⁴, Yuichi Furuyama⁵,
Masahiro Kishida⁶, Hideki Matsune⁶

¹ Technova Inc., 100-0011 Japan,

² Research Center for Electron Photon Science, Tohoku University, 982-0826 Japan,

³ Research Division, Nissan Motor Co., Ltd., 237-8523 Japan,

⁴ Green Mobility Research Institute, Institutes of Innovation for Future Society,
Nagoya University, 464-8603 Japan,

⁵ Graduate School of Maritime Sciences, Kobe University, 658-0022 Japan,

⁶ Graduate School of Engineering, Kyushu University, 819-0395 Japan

E-mail: kitamuraakira3@gmail.com

Abstract Anomalous heat effect by interaction of hydrogen isotope gas and nanoparticles supported by zirconia, PdNi₁₀/ZrO₂ (“PNZ6” and “PNZ6r”) and PdNi₇/ZrO₂ (“PNZ7k”), has been examined. Excess power of 3 ~ 24 W from PNZ6 at elevated temperature of 200 ~ 300 °C continued for several weeks. The PNZ6 and PNZ6r samples with Pd/Ni=1/10 generated much higher excess power than PNZ7k with Pd/Ni=1/7. The Pd/Ni ratio is one of the key factors to increase the excess power. The maximum phase-averaged sorption energy, $\eta_{av,j}$, exceeded 270 keV/D, and the integrated excess energy, E_a , reached 1 keV/Pd·Ni. It is impossible to attribute the excess energy to any chemical reaction; it is possibly due to some unidentified radiation-free nuclear process.

Index Terms – Zirconia supported nanoparticles, Pd-Ni/ZrO₂, hydrogen isotope gas, absorption and desorption, excess power, sorption energy of 270 keV/D.

I. INTRODUCTION

There have been increasing interests in experiments of hydrogen-gas charged nickel-based nano-composite samples for excess power generation, owing to higher availability of nickel than palladium. A Ni-Cu-Mn alloy thin wire, for example, has been examined extensively by Celani et al. ^[1]. In addition, a number of entrepreneurs are publicizing their own “products” of nano-fabricated samples on web sites with undisclosed details, and therefore with little scientific corroboration ^[e.g., 2 – 3]. Among them, replication experiments of the Rossi-type reactors have been performed by several researchers ^[4 – 7], which seemingly appears to show unignorable reproducibility of the Rossi method. However, little is known about the accuracy of the calorimetry and the mechanism of the claimed anomalously large energy production.

On the basis of the 8 year-long (2008-2015) series of study on anomalous heat effects by interaction of metal nanoparticles and D(H)-gas under the collaboration of Technova Inc. and Kobe University, a collaborative research project has begun aiming at a new CO₂-free, distributed energy source ^[8]. This new project on MHE (Metal-Hydrogen Energy) was started on October 2015 under the collaboration of six Japanese organizations, one of which the individual author of the present paper belongs to. The

results of the early-stage research program were reported in 20th International Conference on Condensed Matter Nuclear Science (ICCF20) [9, 10], 17th Meeting of Japan CF-research Society (JCF17) [11, 12] and 12th International Workshop on Anomalies in Hydrogen Loaded Metals [13, 14].

In the present work, we report results of observation of anomalous heat effect (AHE) by interaction of hydrogen isotope gas and zirconia-supported Pd-Ni nanocomposite samples done as the collaborative work using the experimental apparatus installed at Kobe University [15 - 18]. The system has a reaction chamber containing the sample with a capacity of 500 cc, and an oil-flow-calorimetry system capable of working at elevated temperatures up to 300 °C with use of a liquid hydrocarbon coolant, Barreltherm-400. The samples tested so far as the collaborative work include zirconia-supported PdNi_x nanoparticles (“PNZ”), where *x* is 7 or 10. In the present paper, heat-generation characteristics of PNZ samples with different *x*, under rather constant pressure condition after D(H)-absorption (or during effectively net desorption) process are discussed.

II. EXPERIMENTAL PROCEDURE AND SAMPLES

The PNZ samples, PNZ6 and PNZ7k, were prepared by the melt-spinning method similar to that used in ref. [19]. The alloy-compounds of Pd_{0.044}Ni_{0.306}Zr_{0.65} were prepared by arc-melting of the component metal blocks. The alloys were melted again by RF heating, and rapidly solidified with a melt-spinning machine to make ribbon-like thin sheets of amorphous Pd_{0.044}Ni_{0.306}Zr_{0.65} compounds. The thin sheets were calcined in air at a temperature of 450 °C for 60 hours, during which the preferential formation of ZrO₂ supporter zone with isolated distribution of nano-structure zones of PdNi_x is expected. They were then pounded in a mortar to make the sample particles with diameter of several to tens of μm.

The specifications of the samples are tabulated in Table 1. Those of the PNZ6r sample, which is the reused PNZ6 after re-oxidation (re-calcined PNZ6), are also shown in the figure for comparison. Atomic ratio of Pd/Ni was 1/7 for PNZ7k as for other PNZ samples tested so far [8, 15, 17, 18], while that for PNZ6 (and therefore for PNZ6r) was chosen to be 1/10 to see the effect of the Pd/Ni ratio variation on the excess heat magnitude. The oxygen content was evaluated from the weight difference before and after the calcination/re-calcination. The ZrO₂ filler powder is of 1-mm diameter zirconia particles. About 95% of 500 cc volume of the reaction chamber was filled with the zirconia filler, and only about 5% was occupied by the mixed PNZ test sample for AHE measurement.

Table 1. Atomic composition of PNZ6, PNZ6r and PNZ7k sample

Sample	Mass (g)	Molar ratio				ZrO ₂ filler mass (g)
		Ni	Pd	Zr	O	
PNZ6	124.2	0.318	0.032	0.650	0.240	1377
calcined at 450°C for 60h		10 : 1				
PNZ6r	131.9	0.318	0.032	0.650	1.03	1378
recalcined at 450°C for 60h		10 : 1				
PNZ7k	99.8	0.306	0.044	0.650	0.274	1531
calcined at 450°C for 60h		7 : 1				

ICP-AES and XRD analyses for some other PNZ samples, PNZ3, PNZ3r and PNZ4, other than those used in the present work were done at Nissan Motor Co. Ltd., Kyushu Univ., and Nagoya Univ. independently. Many interesting features including crystalline phases of NiZr₂, ZrO₂, etc. have been revealed, which will be published independently elsewhere.

STEM/EDS analyses for PNZ3, PNZ3r and PNZ4 samples (Pd/Ni = 1/7 for these samples) done at Kobe Univ. showed interesting features of nano-structure of the PNZ samples: (1) Most Pd and Ni atoms occupy the same position. (2) After absorption runs, NiZr₂ decreased, and ZrO₂ increased. (3) After re-calcination, the apparent majority became ZrO₂ + NiO + PdO [8, 18].

For the present samples, PNZ6, PNZ6r and PNZ7k, neither ERD, ICP-AES nor STEM/EDS were performed. However, there is no reason to assume characteristics different from PNZ3, PNZ3r and PNZ4 samples for formation of nano-structure.

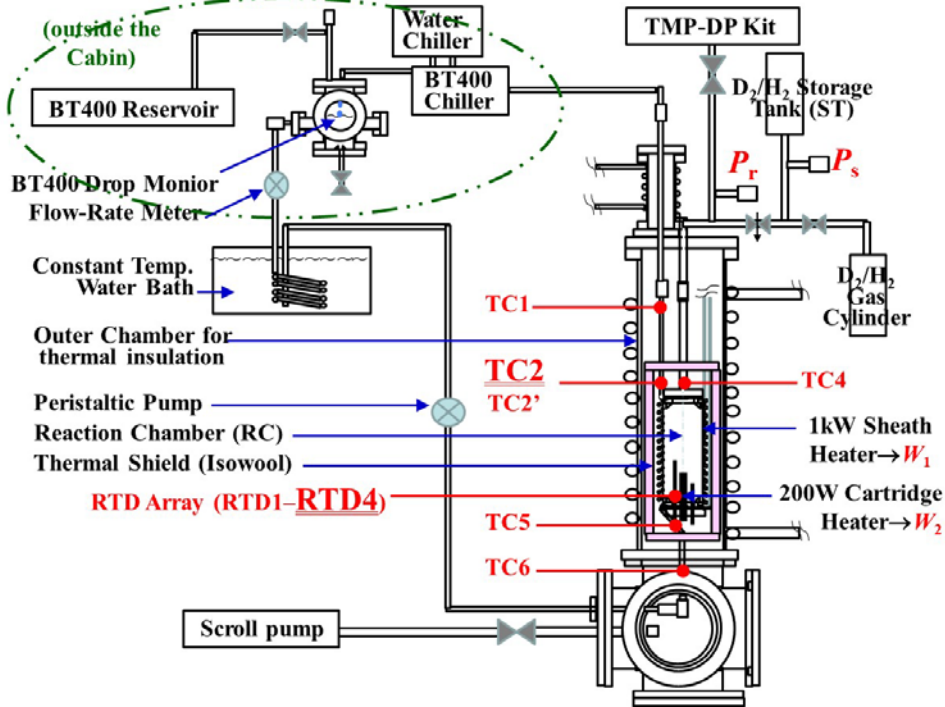


Fig. 1. Schematic of C₁ MHE-experimental system equipped with oil-flow-calorimetry system with flow-rate-monitors and dual heaters mounted on the reaction chamber (RC).

A schematic of the D(H)-gas-charging-calorimetry system C₁ is shown in Fig. 1. Refer to the references [9, 11] for detailed description of the system. Calibration of the flow calorimetry with a flow rate of 20 cc/min was performed using the 1500-g pure ZrO₂ filler. The heat conversion coefficient from the power to the oil-outlet temperature T_{C2} at TC2, dT_{C2}/dW = 1.57 °C/W or 1.0 °C/W, was obtained at room temperature (RT) or at 300 °C, respectively. The heat recovery rate, 0.88 – 0.83 in the temperature range from RT to 300 °C, was calculated by

$$R_h = F \cdot \rho \cdot C \cdot (T_{C2} - T_{C6}) / (W_1 + W_2), \quad (1)$$

where F , ρ and C are the flow rate, the mass density and the specific heat capacity, respectively, of the coolant BarrelTherm-400 (BT400), Matsumura Oil Co. Ltd., and W_1 and W_2 the power of the outer sheath heater (#1) and the inner cartridge heater (#2), respectively. The parameter α is determined empirically as follows. A correction factor for the flow rate fluctuation $\Delta F (= F - F_0)$ to be subtracted from T_{C2} is derived from eq. (1);

$$\Delta T_{C2} = (dT_{C2}/dF) \cdot \Delta F = (-\Delta F/F) \cdot (W_1 + W_2) \cdot (dT_{C2}/dW) \cdot \alpha. \quad (2)$$

The correction is applied to T_{C2} for some samples or gas species to determine α , so that the corrected temperature is not unreasonable, not giving negative excess temperature, or giving null excess for the Ar filling run, in the flow rate range of $0.825 \leq F/F_0 \leq 1$ for $F_0 = 20$ cc/min;

$$\alpha = 1.9 \times 10^{-2} \cdot \exp[4.0 \cdot (F/F_0)]. \quad (3)$$

The calibration run serves also as a control run giving reference values of the temperatures, the flow rate of BT400 and the heater power for foreground runs using the zirconia-supported samples with the pure ZrO_2 filler. Comparing the temperatures in the foreground and background runs, the excess power will be calculated using the heat conversion coefficient mentioned above.

III. RESULTS AND DISCUSSION

(3-1) D(H)-Absorption

Deuterium (D) absorption runs, PNZ6#1, #2, #3 and #4, were performed after vacuum baking (#0) for more than 30 hours at RTD and TC2 temperatures of 200 - 300 °C with the heater power of $(W_1 + W_2) = (69 + 20) \sim (124 + 30)$ W and with the BT400 flow rate of 20 cc/min. The temperature history in the D-PNZ6#0 through #4 is shown in Fig. 2. Each time the heater power was varied, the phase number is advanced; #1-1 for D_2 introduction with the heater power of (0+0) W, #1-2 for (20+10) W, #1-3 for (30+20) W, and so on. At the end of each run, the heated sample was outgassed (“OG” phase) by evacuating the reaction chamber (RC), and the run number is advanced for the succeeding run started with filling of the fresh D_2 gas.

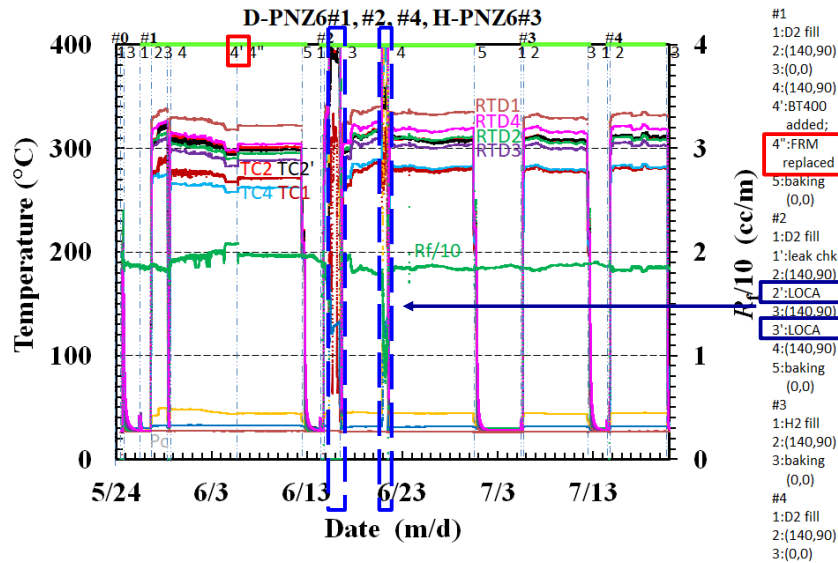


Fig. 2. Evolution of temperature and oil flow rate R_f in PNZ6#0 through #4 runs.

In the figure also shown is the variation of the flow rate R_f of BT400. Although R_f has rather large fluctuation of $\sim 10\%$, the temperature variation due to the fluctuation of R_f is properly corrected for by eq. (2). In the #1 run, there was a trip of the flow-rate-meter (FRM). Then it was replaced with new one. Another trouble we encountered twice was the loss-of-coolant accident (LOCA) at #2-2' and #2-3' phases. In spite of these troubles, we observed rather stable temperature evolution giving large excess power.

In fig. 3 are shown the pressures at the RC and at the storage tube (ST), P_r and P_s , respectively, and the apparent loading ratio $L_M \equiv (D/M)$ or (H/M) , *i.e.*, the number of hydrogen isotope atoms lost from the gas phase relative to the number of metal atoms (Pd and Ni in PNZ runs). The loading ratio is calculated from the values of P_r and P_s , and volumes of the RC and the ST with a correction for the temperature based on the Boyle-Charles' law using the averaged temperature of four RTD's.

It should be noted that the apparent loading ratio L_M reaching 3.5 was exceptionally large in the #1-1 RT phase. It decreased to below 3.0 with elevating the temperature in #1-2 due to desorption. Then it increased gradually due to unexpected leakage of D_2 gas from the RT flanges. The large leakage continued until it was partly fixed at the end of the #2-3' phase, after which the leakage became much smaller. However, the leakage has little influence on L_M in the RT phases, # n -1 ($n = 1 \sim 4$).

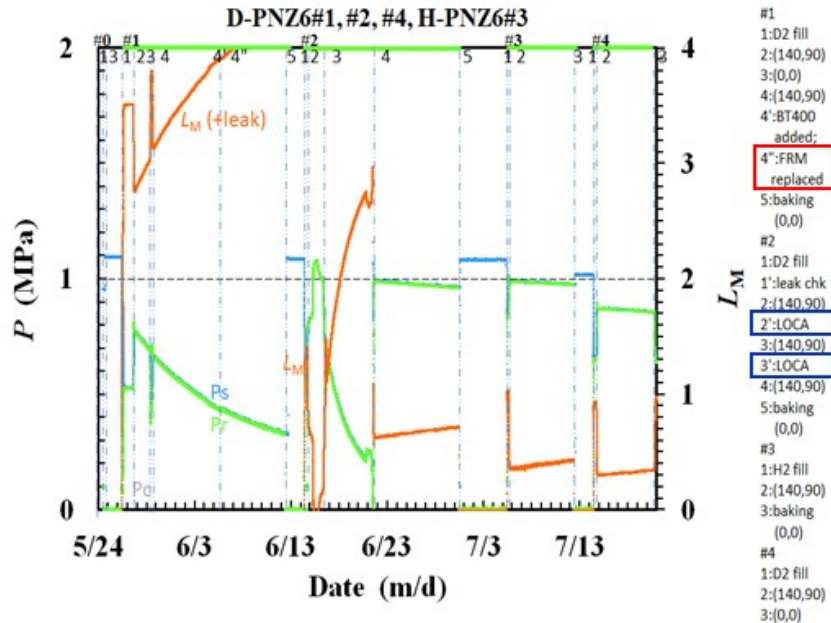
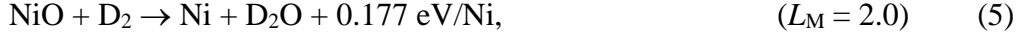


Fig. 3. Evolution of hydrogen loading ratio $L_M (=D/M)$ and D(H)-gas pressure in PNZ6#1~#4 runs.

The variation of L_M with the leakage component subtracted is briefly discussed below. The sample after #0 baking is assumed to be composed of ZrO_2 , $NiZr_2$, NiO and PdO based on the XRD measurements. The possible sources of D consumption are reduction of oxides, (4) and (5) below, absorption by Pd and Ni, (6) and (7), and absorption by $NiZr_2$, (8);





In elevated temperature phases #1- n ($n \geq 2$), desorption of D (reversed (6), (7) and (8)) would proceed, which makes L_M decrease.

At the end of the #1 run the sample was degassed by evacuating the RC at elevated temperature. By this procedure the gases produced by the reactions, D_2O ((4), (5)) and D_2 ((6), (7), (8)) are removed from the system. Then the sample composition after the #1 baking is thought to be ZrO_2 , NiZr_2 , $\text{NiZr}_2\text{D}_{c'}$ and reduced metals ($\text{Ni} + \text{Pd}$). Here it is assumed that NiZr_2D_c and PdD_aNiD_b lose D partially during desorption under elevated temperatures; only a part of NiZr_2D_c turning back to NiZr_2 and/or $\text{NiZr}_2\text{D}_{c'}$ ($c' < c$), and similarly for PdD_aNiD_b . This together with the absence of the oxides would be one of the possible reasons why the D consumption in the #2-1 phase drastically decreased compared with that in the #1-1.

(3-2) Heat evolution at RT

The initial bursts of heat are observed on the RTD and TC traces at the beginning of the #1-1 phase at RT. Figure 4 shows the thermal power calculated from the temperature evolution in the #1-1 phase with the conversion factor mentioned above. The heat evolution has two peaks, simply because the D_2 gas was resupplied to the storage tube at 3.9 h after the initial introduction of D_2 gas. By the resupply the pressure of D_2 in the ST and therefore the flow rate of D_2 was increased to enhance the rate of heat evolution associated with absorption of D_2 .

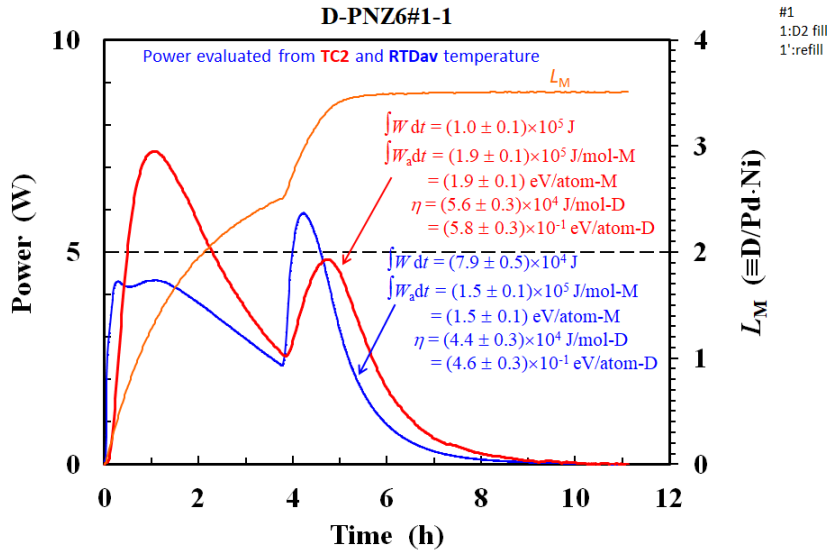


Fig. 4. Thermal power and deuterium loading ratio in the RT phase of the virgin sample run, D-PNZ6#1-1.

The hump at TC2 is time-integrated to calculate an emerging energy per an absorbent atom,

$$E_a = \int_0^t W_a dt, \quad (9)$$

where W_a is the power per an adsorbent atom, Pd and Ni in the present case. The energy E_a is calculated to be 1.9 ± 0.1 eV/atom-Pd. This is rather large in view of the hydrogen absorption energy of about 0.2 eV/atom-Pd for bulk crystalline Pd. The energy E_a is divided by L_M to obtain the specific energy per D atom adsorbed/absorbed or lost from the gas phase, $\eta \equiv E_a/L_M = (5.8 \pm 0.3) \times 10^{-1}$ eV/M, averaged over the #1-1 phase. Similarly, E_a and η are calculated for # n -1, where n is the integer representing the run number. Those together with L_M are summarized in Fig. 5, and compared with those for PNZ6r and PNZ7k samples.

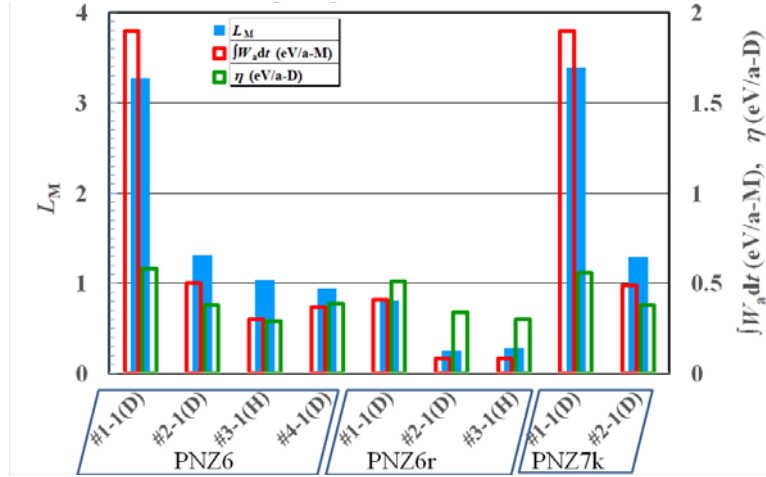


Fig. 5. Comparison of loading ratio and specific absorption energies in room temperature phases of PNZ6#1-1 through PNZ7k#2-1 runs.

Some conclusions are deduced from the figure. First of all, PNZ7k is similar to PNZ6 in regard to these quantities. The reproducibility is rather good.

Secondly, we notice the exceptionally large value of L_M at #1-1, and gradual decrease of L_M in the following phases. The difference between L_M in #1-1 and that in #2-1 is almost 2. As has been partly discussed in the preceding subsection, possible reasons for this large difference are the following. (1) In the elevated temperature phases only a part of NiZr_2D_c liberate D_2 turning back to NiZr_2 or $\text{NiZr}_2\text{D}_{c'}$ ($c' < c$). The liberated D_2 gas is removed by evacuation at the end of the #1 run. (2) Similarly, only a part of $\text{PdD}_a\text{-NiD}_b$ could liberate D_2 turning back to $\text{PdD}_a\text{-NiD}_b$. (3) The oxides $\text{PdO}\cdot\text{NiO}$ to be deduced to metallic $\text{Pd}\cdot\text{Ni}$ by consuming D_2 is absent or very few in the #2 run.

Third, the specific absorption energies per D atom, η , have essentially the same value (0.3 ~ 0.4 eV/D) in $\text{PNZ6}\#n-1$, where $n \geq 2$. This infers that the underlying physics is the same in the $\text{PNZ6}\#n-1$ phases. In other words, this means that the reduction of $\text{PdO}\cdot\text{NiO}$, if any, was almost completed in #1-1, and that the values of η in # n -1 ($n \geq 2$) are the intrinsic ones for the sample. Possible processes responsible to this are the deuterium absorption by Pd-Ni, eqs. (6) and (7), and by NiZr_2 , eq. (8). Gradual decrease of L_M and E_a suggests that decomposition of NiZr_2 and/or some structural degradation of the Pd-Ni nanostructure are proceeding. The intrinsic $\eta \sim 0.8$ is much larger than that for the bulk Pd (~ 0.2 eV/a-D). Possible reasons for this are the following; (1) The absorption energy E_{NiZr_2} in eq. (8) is rather large. (2) It might be possible that the absorption energies (6)·(7) become larger when Pd and Ni form

nanocomposites. (3) It might also be possible that some unknown reactions other than absorption occur in the Pd·Ni nanocomposites. In #1-3 with the filling gas of H₂, η is decreased by about 25% possibly due to the isotope effect. Anyway, it is difficult to discuss further these points before knowing the composition quantitatively.

Fourth, The PNZ6r runs have similar variation of L_M and E_a but with smaller amplitude. It appears that the numbers of the absorbers, NiZr₂ and NiO, are reduced in comparison with the PNZ6. It seems that, by re-calcination, some fraction of NiZr₂ are likely to be decomposed to ZrO₂ and Ni/NiO, and some fraction of Pd·Ni nanostructure might be changed to different one relatively inactive in regard to absorption.

(3-3) Heat evolution at ET

Next, we discuss the oil-outlet temperature T_{C2} in the elevated temperature phases in the PNZ6 runs, T_{C2} (PNZ6) (the red line in Fig. 6), in comparison with T_{C2} (ZrO₂) in the calibration/control run using the zirconia powder (the black line in Fig. 6). As is shown, T_{C2} (PNZ6) is higher than T_{C2} (ZrO₂) in most elevated temperature phases. When we take into account the fluctuation of the heater power and the flow rate as seen in Fig. 2, and apply the correction according to eq. (2), we obtain the curve shown as the green line in Fig.6.

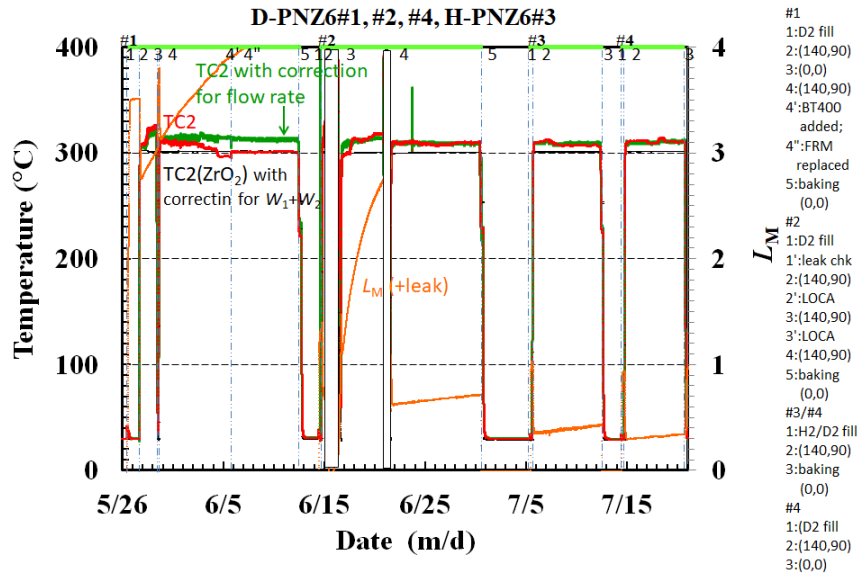


Fig. 6. Difference of TC2 temperature between the foreground (PNZ6) run and the blank (zirconia) run.

The difference is converted to excess power, W_{ex} , by dividing it by dT_{C2}/dW , and shown in Fig. 7. The excess power of 10 ~ 24 W is rather large. When we take into account the systematic error of ± 2.3 W determined from fluctuations recorded in PSf1 runs [11], the maximum excess power is more than one order of magnitude higher than the error range. In the PNZ6 sample powder some anomalous effect is induced to generate excess power in all phases with the elevated temperature of 300 ~ 340 °C at RTD1 ~ RTD4.

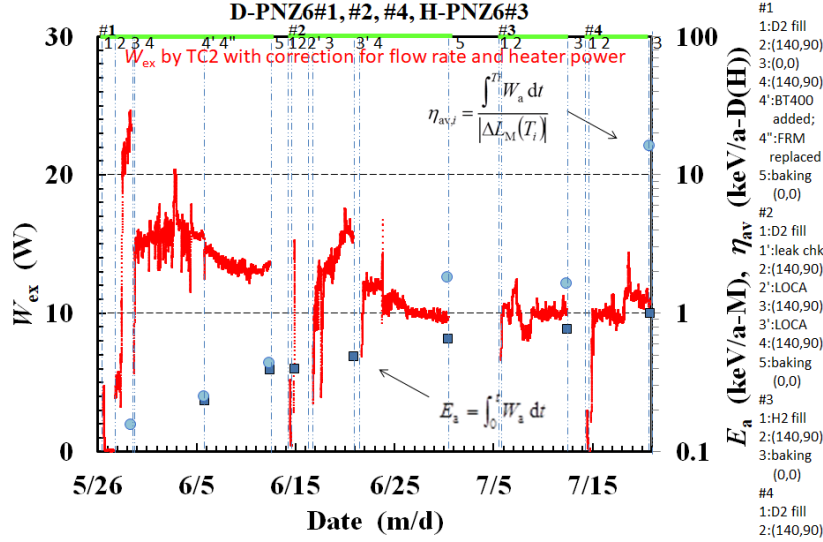


Fig. 7. Excess power, W_{ex} , integrated excess heat per metal atom, E_a (keV/M), and phase-averaged sorption energy per hydrogen isotope atom absorbed/desorbed, $\eta_{\text{av},i}$ (keV/D(H)), in RT and ET phases evaluated by TC2 temperature

The phase-averaged sorption energy, $\eta_{\text{av},i}$ (closed circles), and the integrated excess energy per an adsorbent atom, E_a (integrated W_{ex} per adsorbent atom; closed squares), in the elevated temperature phases are also plotted in Fig. 7. It should be noted that $\eta_{\text{av},i}$ is defined as E_a divided by the absolute value of ΔL_M , the increment of adsorbed/absorbed or desorbed deuterium atoms in the relevant phase;

$$\eta_{\text{av},i} \equiv \frac{\int_0^{T_i} W_a dt}{|\Delta L_M(T_i)|}, \quad (10)$$

The absolute value is taken to keep $\eta_{\text{av},i}$ positive under desorption. This is because we assume that the exothermic event could occur along with hydrogen isotope displacement under both absorption and desorption. The maximum value of $\eta_{\text{av},i}$ exceeds 10 keV/D, and the integrated output energy E_a reaches 1 keV/Pd·Ni.

The definition of $\eta_{\text{av},i}$ is rather problematic, since the real number of the hydrogen atoms getting in and out of the surfaces of the nanoparticles is not always represented by $|\Delta L_M|$ in the denominator of eq. (10). However, even if we divide E_a by the total amount of D absorbed in each run, L_M , to evaluate the integrated output energy per an D atom participating in the absorption, the energy is still far beyond the value explainable by any chemical reaction; $E_a/L_M = 460 \text{ eV/D} = 44 \text{ MJ/mol-D}$ in the D-PNZ6#4 run. The large values of the excess energy suggest the nuclear origin of the excess heat.

It is important to note that the sudden increase of W_{ex} in the #1-2 phase is really spontaneous. Figure 8 shows the unexpected, unintended evolution of excess power in the #1-2 phase having no correlation with fluctuation of the flow rate nor the input heater power. Figure 9 shows the temperatures at other TCs and RTDs during the same period of time. The unexpected, unintended evolution of excess power appears to originate in the peripheral region of RC. This is because the step-like increases of

temperature are observed with much smaller amplitude in RTDs which are relatively insensitive to the temperature at the peripheral region. The excess power in the #1-2 phase reaching 24 W is largest among all sample runs tested so far.

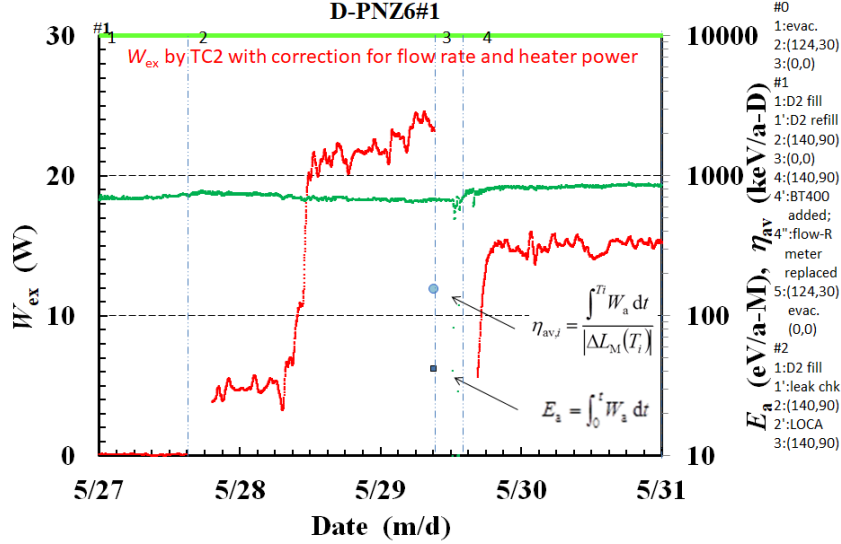


Fig. 8. Unexpected, unintended evolution of excess power with no correlation with the flow rate.

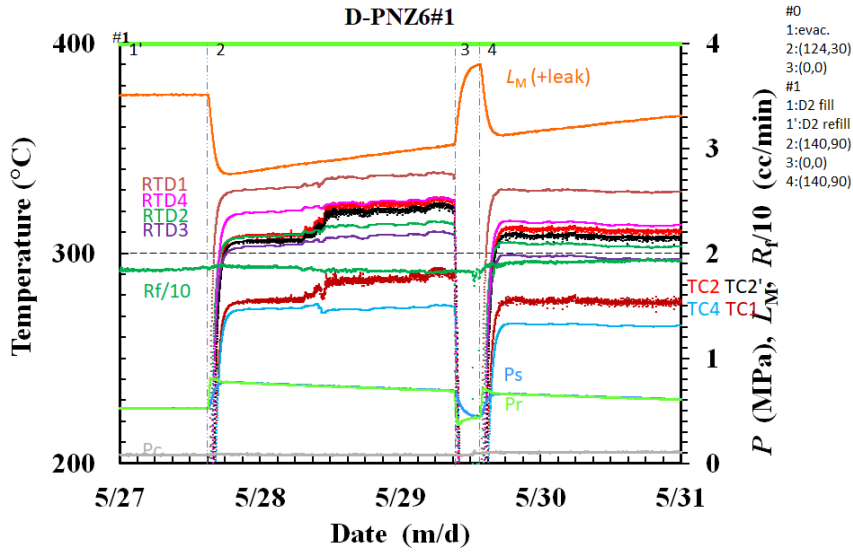


Fig. 9. Temperatures at TCs and RTDs, the loading ratio L_M and flow rate R_f , when the large excess power emerged.

The PNZ6 sample was re-calcined after finishing the PNZ6#4 run. The sample is called PNZ6r, and similar sequence of heater power application was given to the PNZ6r sample. As might be supposed from L_M for RT phases shown in Fig. 5, deuterium absorption is weaker than PNZ6; L_M in the ET phases, #1-2 through #1-5, is about 0.5 and smaller than 0.3 in #2-2 ~ 4 and #3-2 phases. Evolution of the excess power, W_{ex} , the integrated excess energy per metal atom, E_a , and the phase-averaged sorption energy per D atom absorbed/desorbed, $\eta_{av,i}$, in the PNZ6r runs are shown in Fig. 10.

We see again rather large value of W_{ex} stably ranging from 5 to 10 W. Very large values of $\eta_{av,i}$ with the maximum value of 270 keV/D, and/or even the conservatively defined integrated excess energy $E_a/L_M = 85$ MJ/mol-D in the PNZ6r#1 run, make it realistic to assume nuclear origin of the excess heat.

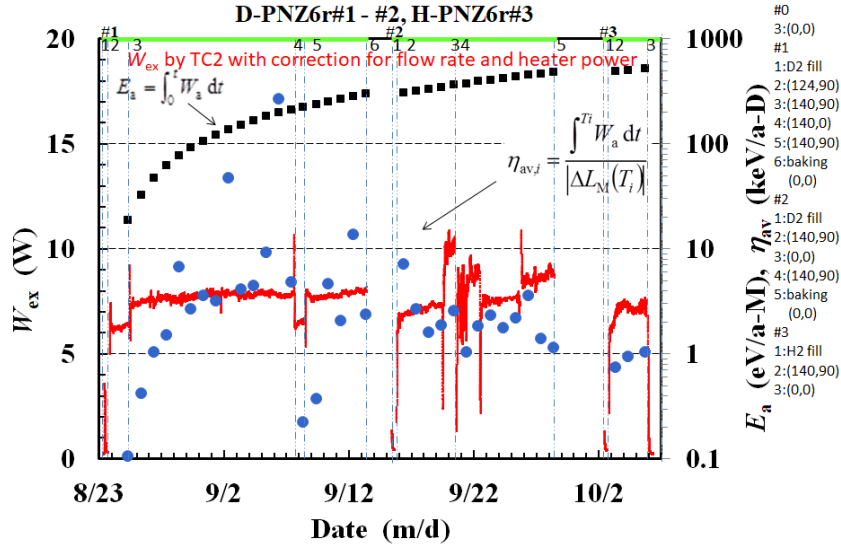


Fig. 10. Excess power, W_{ex} , and excess energies E_a (keV/M) and $\eta_{av,j}$ (keV/D(H)), in PNZ6r runs.

Figure 11 shows peculiar evolution of temperature observed in the PNZ6r#1-2 phase. Relatively large humps are recorded in the RTD1 and RTD2 traces. The figure also shows desorption under elevated temperature in #1-2 similar to other samples, but with exceptionally large time constant. The reason for these phenomena is not known. However, it is very interesting to see that large positive excess power evolution was generated under the net desorption process as shown in Fig. 10 and Fig. 11. This effect seems to infer that nuclear-like reaction sites exist in the near-surface of PdNi_x nano-composites.

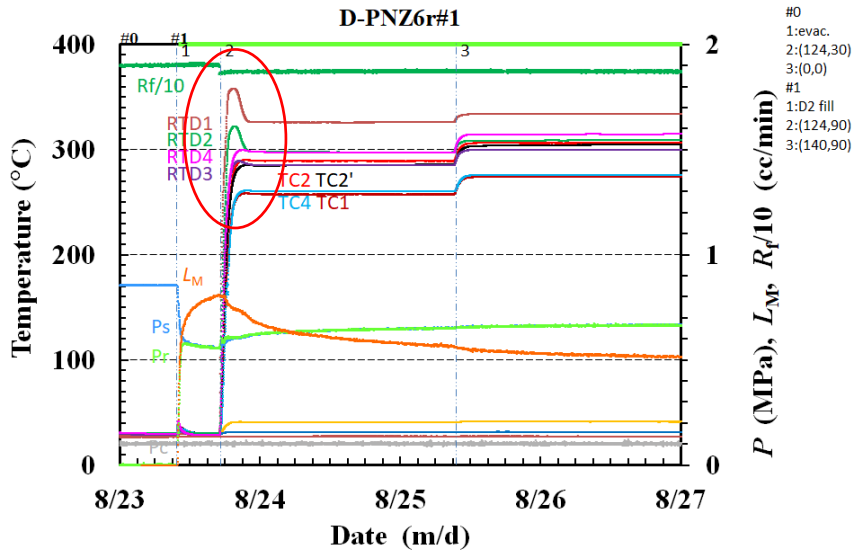


Fig. 11. Peculiar evolution of temperature in the D-PNZ6r#1-2 phase.

Finally, the excess power characteristics of PNZ7k sample with the atomic ratio of Pd/Ni = 1/7. As has been mentioned earlier, this sample in the RT phases shows characteristics very similar to those for the PNZ6 sample. The similarity is also true for L_M in the ET phases but without leakage. However, there is a large difference in excess power and energies. These are shown in Fig. 12. The excess power W_{ex} and accordingly the integrated excess energy E_a are appreciably small compared with that for PNZ6 and PNZ6r. As for the phase-averaged sorption energy, $\eta_{av,i}$, the values are not very small, yet remarkably large values are not observed. From these facts we conclude that the atomic ratio of binary adsorbent metal in the sample is one of the key factors to increase the excess power. The smaller the ratio of the minority species to the majority, the larger the excess power. However, we know that single-element nanoparticle sample never produce excess heat in ET phases^[11]. We have to look for the most suitable ratio.

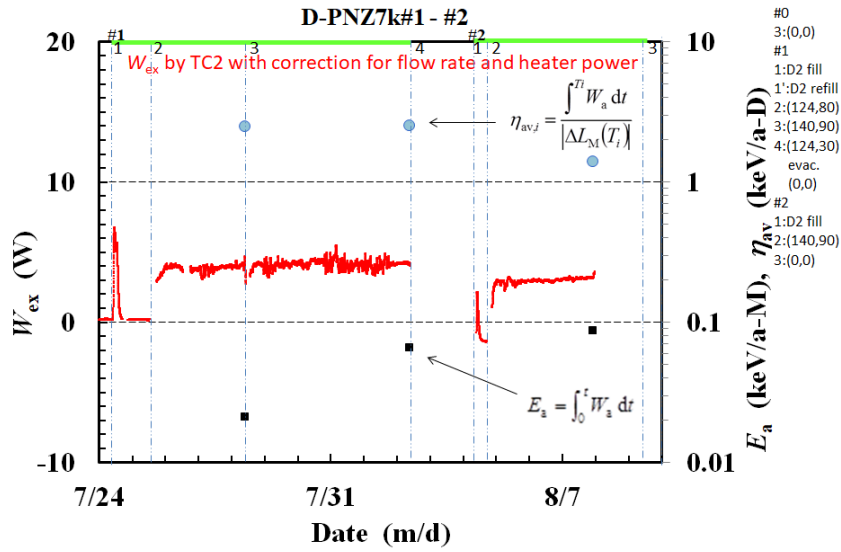


Fig. 12. Excess power, W_{ex} , and excess energies E_a (keV/M) and $\eta_{av,i}$ (keV/D(H)), in PNZ7k runs.

(3-4) Radiations

Finally, radiation measurements are discussed. An example of the result of measurements of γ -ray counting rate and neutron dose rate is shown in Fig. 13. The γ -ray counting rate and the neutron dose rate are steady with rather large fluctuation, except for a period with high neutron dose rate in middle July. However, the period agrees with the period when the accelerator in the next room was operated in the neutron emitting mode. We conclude that no observable level of hard radiation accompanies the excess heat at least up to the power level observed in the present work.

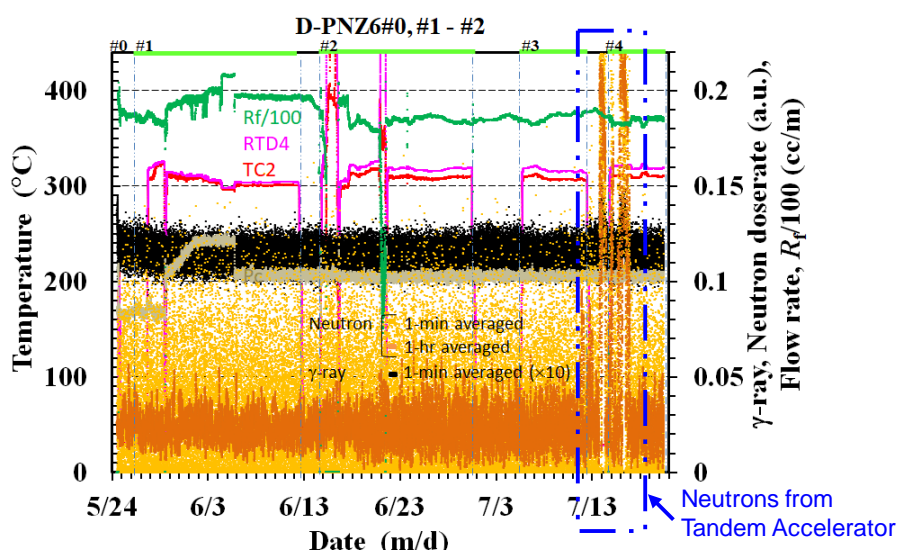


Fig. 13. Radiations and temperatures at TC2 and RTD4 in PNZ6 runs.

IV. SUMMARY AND CONCLUDING REMARKS

Hydrogen isotope absorption and heat evolution have been examined for three kinds of ZrO₂-supported Pd·Ni nanocomposites, PNZ6, PNZ6r, and PNZ7k. The results are summarized as follows;

- (1) Excess power of 3~24W at elevated temperature of 200~300°C continued for several weeks.
- (2) PNZ6 and PNZ6r samples with Pd/Ni=1/10 generated much higher excess power than PNZ7k with Pd/Ni=1/7. The Pd/Ni ratio is one of the keys to increase the excess power.
- (3) The maximum phase-averaged sorption energy, $\eta_{av,i}$, exceeded 270 keV/D (26 GJ/mol-D), and the integrated excess energy, E_a , reached 1 keV/Pd·Ni (100 MJ/mol-M).
- (4) It is impossible to attribute the excess energy to any chemical reaction; it is possibly due to radiation-free nuclear process.
- (5) The anomalous heat effect was observed with very small amount of D(H) transfer in both direction of net absorption and net desorption. It is conceived that this might be a hint for AHE generation sites and some nuclear mechanism in the binary nano-metal composite samples.

References

- [1] F. Celani, E. F. Marano, B. Ortenzi, S. Pella, S. Bartalucci, F. Micciulla, S. Bellucci, A. Spallone, A. Nuvoli, E. Purchi, M. Nakamura, E. Righi, G. Trenta, G. L. Zangari, and A. Ovidi, "Cu-Ni-Mn alloy wires, with improved sub-micrometric surfaces, used as LENR device by new transparent, dissipation-type, calorimeter", J. Condensed Matter Nucl. Sci. **13** (2014) 56-67.
- [2] F. Piantelli / Nichenergy; <http://e-catsite.com/2012/06/15/piantelli-moves-closer-to-commercialization/>.
- [3] A. Rossi / Leonardo Corporation; <http://ecat.com/>.

- [4] G. Levi, E. Foschi, B. Höistad, R. Pettersson, L. Tegner and H. Essen., <http://www.sifferkoll.se/sifferkoll/wp-content/uploads/2014/10/LuganoReportSubmit.pdf>.
- [5] A. G. Parkhomov, *International Journal of Unconventional Science*, **6**(2) (2014) 57-61; *ibid.* **7**(3) (2015) 68-72; *ibid.* **8**(3) (2015) 34-39.
- [6] S. Jiang, <http://ja.scribd.com/doc/267085905/New-Result-on-Anomalous-Heat-Production-in-Hydrogen-loaded-Metals-at-High-Temperature>, (2015).
- [7] J. Cole, <http://www.lenr-coldfusion.com/2015/04/16/experiment-generates-apparent-excess-heat/>, (2015).
- [8] A. Takahashi, A. Kitamura, K. Takahashi, R. Seto, T. Yokose, A. Taniike and Y. Furuyama, "Anomalous Heat Effects by Interaction of Nano-metals and D(H)-gas", published in *Proc. ICCF20* (2016), pp. 13-25, Tohoku University) .
- [9] Akira Kitamura, Akito Takahashi, Koh Takahashi, Reiko Seto, Yuki Matsuda, Yasuhiro Iwamura, Takehiko Itoh, Jirohta Kasagi, Masanori Nakamura, Masanobu Uchimura, Hidekazu Takahashi, Tatsumi Hioki, Tomoyoshi Motohiro, Yuichi Furuyama, Masahiro Kishida, "Collaborative Examination on Anomalous Heat Effect Using Nickel-Based Binary Nanocomposites Supported by Zirconia", *J. Condensed Matter Nucl. Sci.* **24** (Proc. ICCF20) (2017) 202 - 213.
- [10] Y. Iwamura, T. Itoh, J. Kasagi, A. Kitamura, A. Takahashi and K. Takahashi, "Replication Experiments at Tohoku University on Anomalous Heat Generation Using Nickel-Based Binary Nanocomposites and Hydrogen Isotope Gas", *J. Condensed Matter Nucl. Sci.* **24** (Proc. ICCF20) (2017) 191 - 202.
- [11] A. Kitamura, A. Takahashi, K. Takahashi, R. Seto, T. Hatano, Y. Iwamura, T. Itoh, J. Kasagi, M. Nakamura, M. Uchimura, H. Takahashi, S. Sugitomo, T. Hioki, T. Motohiro, Y. Furuyama, M. Kishida, and H. Matsune, "Heat evolution from silica-supported nano-composite samples under exposure to hydrogen isotope gas", *Proc. JCF17* (2017) 1-14.
- [12] Y. Iwamura, T. Itoh, J. Kasagi, A. Kitamura, A. Takahashi, K. Takahashi, R. Seto, T. Hatano, T. Hioki, T. Motohiro, M. Nakamura, M. Uchimura, H. Takahashi, S. Sugitomo, Y. Furuyama, M. Kishida, and H. Matsune, "Anomalous Heat Generation Experiments Using Metal Nanocomposites and Hydrogen Isotope Gas", *Proc. JCF17* (2017) 15-27.
- [13] Akira Kitamura, Akito Takahashi, Koh Takahashi, Reiko Seto, Takeshi Hatano, Yasuhiro Iwamura, Takehiko Itoh, Jirohta Kasagi, Masanori Nakamura, Masanobu Uchimura, Hidekazu Takahashi, Shunsuke Sumitomo, Tatsumi Hioki, Tomoyoshi Motohiro, Yuichi Furuyama, Masahiro Kishida, and Hideki Matsune, "Effect of Supporter Material on Heat Evolution from Ni-based Nano-Composite Samples under Exposure to Hydrogen Isotope Gas", presented at 12th Int. Workshop on Anomalies in Hydrogen-Loaded Metals, Costigliole d'Asti, Italy, 5-9 June 2017.
- [14] Y. Iwamura, T. Itoh, J. Kasagi, A. Kitamura, A. Takahashi, K. Takahashi, R. Seto, T. Hatano, T. Hioki, T. Motohiro, M. Nakamura, M. Uchimura, H. Takahashi, S. Sugitomo, Y. Furuyama, M. Kishida, and H. Matsune, "Anomalous Heat Generation Experiments Using Metal Nanocomposites and Hydrogen Isotope Gas", presented at 12th Int. Workshop on Anomalies in Hydrogen-Loaded Metals, Costigliole d'Asti, Italy, 5-9 June 2017.
- [15] A. Kitamura, A. Takahashi, R. Seto, Y. Fujita, A. Taniike and Y. Furuyama, "Brief summary of latest experimental results with a mass-flow calorimetry system for

- anomalous heat effect of nano-composite metals under D(H)-gas charging”, *Current Science*, **108**(4) (2015) 589-593.
- [16] A. Kitamura, A. Takahashi, R. Seto, Y. Fujita, A. Taniike and Y. Furuyama, “Comparison of some Ni-based nano-composite samples with respect to excess heat evolution under exposure to hydrogen isotope gases”, *Proc. JCF15* (2015) 1-19.
- [17] A. Kitamura, A. Takahashi, R. Seto, Y. Fujita, A. Taniike, Y. Furuyama, “Effect of Minority Atoms of Binary Ni-Based Nano-Composites on Anomalous Heat Evolution under Hydrogen Absorption”, *J. Condensed Matter Nucl. Sci.* **19** (2016) 135-144 (Proc. ICCF19 (2015)).
- [18] A. Kitamura, E. F. Marano, A. Takahashi, R. Seto, T. Yokose, A. Taniike and Y. Furuyama, “Heat evolution from zirconia-supported Ni-based nano-composite samples under exposure to hydrogen isotope gas”, *Proc. JCF16* (2016) 1-16.
- [19] Y. Arata and Y. Zhang; The special report on research project for creation of new energy; *J. High Temperature Society* 34 (2008) 85-93.